Study of π^- Inclusive Production in γd Interactions with a 7.5-GeV Linearly Polarized Photon Beam

G. Alexander, O. Benary, S. Dagan, J. Gandsman, J. Grunhaus, P. Katz,* A. Levy,† and D.A. Lissauer
Department of Physics and Astronomy, Tel Aviv University, Tel Aviv, Israel
(Received 20 September 1972)

The reaction $\gamma d \to \pi^- +$ anything at 7.5 GeV with a linearly polarized photon beam has been studied. The γn average charge multiplicity was found to be a unit charge less than the γp average charge multiplicity. We have extracted information on the inclusive π^- production in γn reactions using the γp inclusive data. The ratio of π^+ to π^- inclusive production in the target fragmentation region was found to be independent of the beam. Two-particle correlations in both x and y variables are presented.

I. INTRODUCTION

Single-particle inclusive spectra have been studied extensively with different hadronic incoming and outgoing particles.[1] Photoproduction inclusive reactions producing π^- (Ref. 2), π^+, K^+, and K^- (Ref. 3) have also been studied using a hydrogen target. There has been some effort to extract inclusive data from exclusive channels using a deuteron target and hadronic beams,[4] but so far no γd inclusive data have been reported.

In this paper we present the results of a study on the reaction

$$\gamma d \to \pi^- + \text{anything} \tag{1}$$

using a linearly polarized photon beam at 7.5 GeV. Reaction (1), $(\gamma d, \pi^-)$, is composed of three main components: (a) the reaction $(\gamma p, \pi^-)$ with a neutron spectator, (b) $(\gamma n, \pi^-)$ with a proton spectator, and (c) $(\gamma d_c, \pi^-)$, where d_c denotes a deuteron coherent reaction, i.e., there is a deuteron in the final state. The coherent sample (c) is expected to be small in comparison with reactions (a) and (b),[5] and consequently we have analyzed our data assuming

$$(\gamma d, \pi^-) \simeq (\gamma p, \pi^-) + (\gamma n, \pi^-). \tag{2}$$

Experimental procedure and cross-section information are given in Sec. II. In Sec. III, the $(\gamma d, \pi^-)$ inclusive data are presented. Using the existing $(\gamma p, \pi^-)$ data[2] at nearby energies and our $(\gamma d, \pi^-)$ data, we compare in Sec. IV the two reactions and extract information on $(\gamma n, \pi^-)$, using Eq. (2). In Sec. V we present the results of a study of two-particle correlations, which recently became of theoretical interest.[6] Conclusions are given in Sec. VI.

II. EXPERIMENTAL DATA

Approximately 170 000 photographs were taken in an exposure of the deuterium-filled SLAC 82-in. bubble chamber to a nearly monochromatic polarized photon beam[7] at 7.5 GeV. Figure 1 shows the photon spectrum from the measurements of about 5000 e^+e^- pairs, showing the momentum resolution to be $\Delta p/p = \pm 4\%$.

The film was scanned twice for all topologies, and disagreements between the scans were resolved on the scanning table. Scanning efficiency for topologies with ≥ 3 outgoing charged particles was close to 100%, independent of the momenta and angles of the secondary particles. Since two-prong events with a small angle between them are in this experiment mostly e^+e^- pairs, they were measured only in part of the film. Thus, only 70% of the two-prong events were included in the data, as estimated in a Monte Carlo calculation. The events were then measured on conventional digitizing machines, and geometrical reconstruction of the tracks was obtained using the program TVGP. In this way a total of about 8000 events were accepted for physics analysis.

The hadronic cross section can be expressed by the following relation:

$$\sigma_H = \frac{N_H}{N_p}\sigma_p, \tag{3}$$

where N_H and σ_H are respectively the number of hadronic events and the corresponding cross section. N_p and σ_p are the number of pairs and the corresponding pair cross section, which was taken as[8] 20.2 ± 0.1 mb. In this way the γd total hadronic cross section in this experiment was found to be

$$\sigma_T(\gamma d) = 234 \pm 17\ \mu\text{b}.$$

The error in the cross section includes both statistical and systematic errors. Since the zero-prong events could not be detected in this experiment, their cross section was estimated to be less than 5 μb using the value of the one-prong cross section. This value of the total γd cross section is in good agreement with the values measured previously in counter experiments.[9] In Table I we give

TABLE I. γd multiplicity and topological cross sections.

γd multiplicity m	σ_m (μb)	Topology [a] k	σ_k (μb)
3	125.3 ± 9.3	2 prongs [b]	44.1 ± 3.5
		3 prongs	81.2 ± 6.0
5	59.7 ± 4.4	4 prongs	21.0 ± 1.6
		5 prongs	38.7 ± 2.9
7	12.4 ± 1.1	6 prongs	5.1 ± 0.5
		7 prongs	7.3 ± 0.7
9	1.0 ± 0.2	8 prongs	0.35 ± 0.10
		9 prongs	0.65 ± 0.15

[a] Strange particles with visible decay are not included in this table.

[b] Corrected for small-opening-angle events.

the charge multiplicity m, the cross sections σ_m, and the topological cross sections σ_k, where k is the visible charge multiplicity. Note that the charge multiplicity and the visible charge multiplicity are not identical because of invisible proton spectators and invisible deuterons.

The average charge multiplicity of the reaction $(\gamma d, \pi^-)$, defined as

$$\langle m \rangle = \frac{\sum m\sigma_m}{\sigma}, \tag{4}$$

gives a value of 3.6 ± 0.2 at 7.5 GeV. Under the assumption of Eq. (2) we obtain the following relation between the average deuteron charge multiplicity $\langle m\rangle_d$ and the proton ($\langle m\rangle_p$) and neutron ($\langle m\rangle_n$) average charge multiplicities:

$$\sum m\sigma_m \equiv \sigma_d \langle m\rangle_d \simeq \sigma_p \langle m\rangle_p + \sigma_n(\langle m\rangle_n + 1). \tag{5}$$

The total hadronic photoproduction cross section for deuteron, proton, and neutron targets are denoted by σ_d, σ_p, and σ_n, respectively. Note that the last term in Eq. (5), which represents the neutron-induced reactions, has an additional unit charge added to $\langle m\rangle_n$ to account for the presence of a proton spectator in each neutron reaction.

From the SLAC-Berkeley-Tufts (SBT) data[2] we find the interpolated value for $\langle m\rangle_p$ to be 3.5 at 7.5 GeV. Using Eq. (5) and the fact[9] that at this energy $\sigma_n \simeq \sigma_p \simeq \sigma_d/2$ we find $\langle m\rangle_n = 2.7 \pm 0.2$. This value lower than $\langle m\rangle_p$ by one unit of charge. This is due to the fact that the "net" charge multiplicity, [3] i.e., the difference between the final and the initial charge multiplicity, is the same for γp and γn.

III. DATA PRESENTATION

We analyzed our inclusive data in terms of the following variables:

(a) the Feynman variable[10] x, defined in the overall center-of-mass system as

$$x = p^*_{\parallel}/p^*_{\max}, \tag{6}$$

where $p^*_{\parallel}$ is the longitudinal momentum of the observed outgoing particle and $p^*_{\max}$ is the maximum kinematically allowed momentum for that particle;

(b) the longitudinal momentum $p_{\parallel}$ in the laboratory system[11];

(c) the perpendicular momentum $p_{\perp}$ in the c.m. system; and

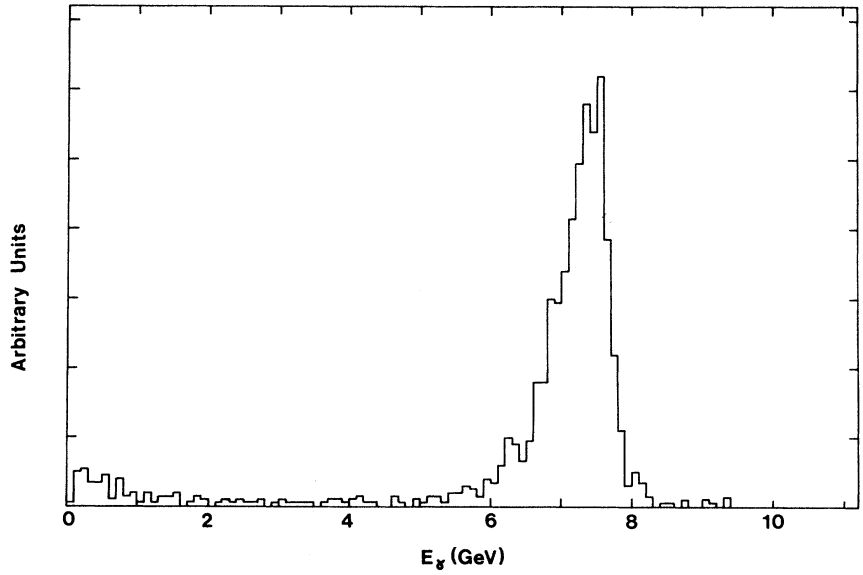

FIG. 1. Photon energy spectra from e^+e^- pair measurements.

(d) the rapidity variable y, defined in the laboratory system as

$$y = \tfrac{1}{2} \ln\left(\frac{E + p_{\parallel}}{E - p_{\parallel}}\right). \tag{7}$$

In the following analysis the over-all c.m. system was defined as the γ-nucleon c.m. system, in accordance with the assumption expressed in Eq. (2).

In Fig. 2 we show the quantity $F(x)$, defined as

$$F(x) = \int_0^{\infty} \frac{E^*}{\pi p^*_{\max}} \frac{d^2\sigma}{dx dp_{\perp}^2} dp_{\perp}^2 \tag{8}$$

as a function of x. The region $x = -1$ ($x = +1$) corresponds to backward- (forward-) going pion, i.e., target (beam) fragmentation region. From the data it is apparent that $F(x)$ reaches a maximum at $x = 0$ (pionization region[1]) and falls off on both sides at different rates, attaining for the ratio $F(+1)/F(-1)$ a value of ~10. For comparison we also show in the same figure the γp data at 9.3 GeV given by the SBT collaboration.[2] (The dashed curve is an approximation to the γp data.)

In Fig. 3 we show the longitudinal-momentum structure function distribution $F(p_{\parallel})$ versus $p_{\parallel}$ in the laboratory system, where

$$F(p_{\parallel}) = \int_0^{\infty} E \frac{d^2\sigma}{dp_{\parallel} dp_{\perp}^2} dp_{\perp}^2 . \tag{9}$$

The structure function rises rapidly from $p_{\parallel} = -0.5$ GeV/c, reaching a maximum in the region of $p_{\parallel}$ ~0.5–1.0 GeV/c followed by a slow decrease to zero at the kinematically allowed limit. In Fig. 4 we show the transverse-momentum structure function distribution $F(p_{\perp}^2)$ versus $p_{\perp}^2$, where

$$F(p_{\perp}^2) = \int_0^{\infty} E \frac{d^2\sigma}{dp_{\parallel} dp_{\perp}^2} dp_{\parallel} . \tag{10}$$

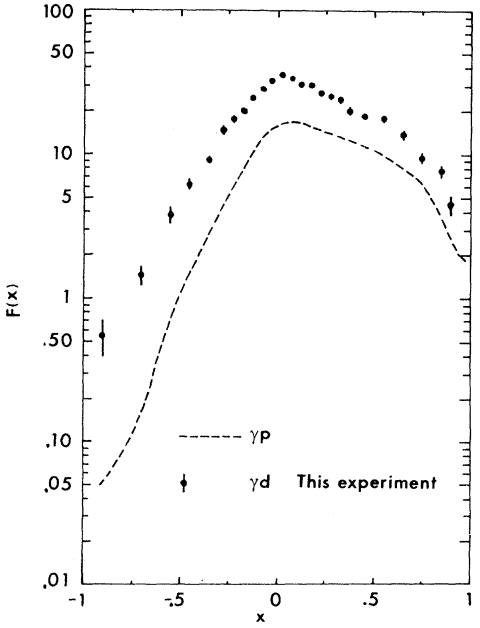

FIG. 2. The structure function $F(x)$ versus x. The dashed line is an approximation of $F(x)$ from the $(\gamma p, \pi^-)$ data at 9.3 GeV.

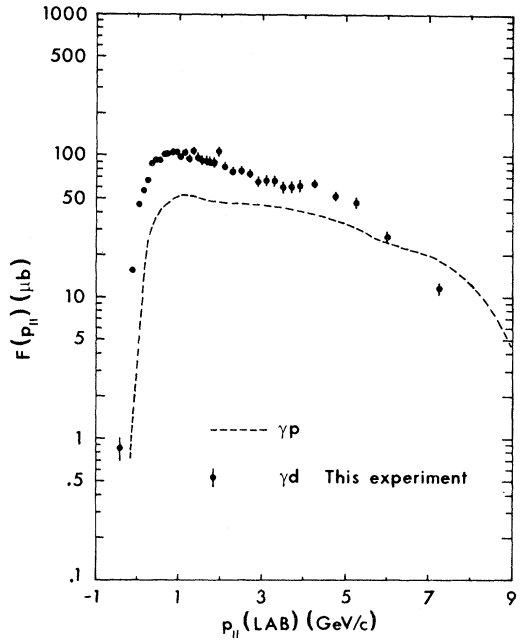

FIG. 3. The structure function $F(p_{\parallel})$ versus $p_{\parallel}$. The dashed line is an approximation of $F(p_{\parallel})$ from the $(\gamma p, \pi^-)$ data at 9.3 GeV.

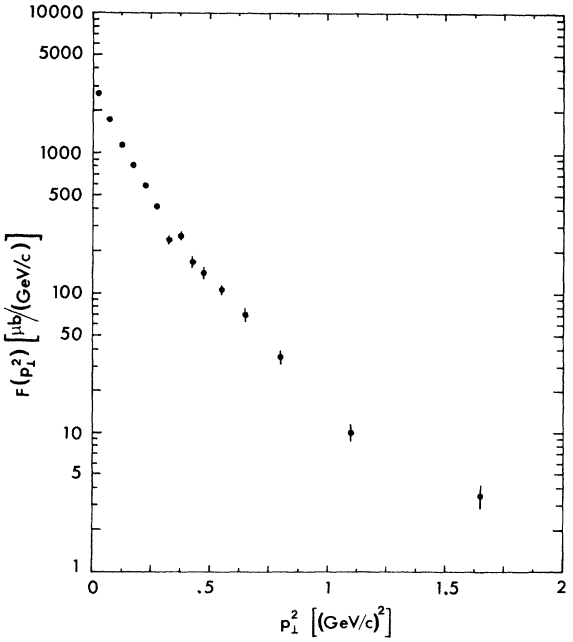

FIG. 4. The structure function $F(p_{\perp}^2)$ versus $p_{\perp}^2$.

The distribution shows exponential decrease at small $p_\perp{}^2$, and at higher $p_\perp{}^2$ values the slope of the distribution changes continually.

In Fig. 5 the rapidity distribution integrated over all $p_\perp{}^2$ is shown. The predicted flat top,[12] which is expected at high incident momentum, is not observed here. The absence of a flat top in a γp experiment[2] at 9.3 GeV was pointed out earlier.

IV. COMPARISON WITH THE $(\gamma p,\pi^-)$ REACTION

Assuming Eq. (2) to be valid, one may extract the $(\gamma n,\pi^-)$ inclusive spectra from $(\gamma d,\pi^-)$ and $(\gamma p,\pi^-)$ data at the same energy. There is no $(\gamma p,\pi^-)$ experiment at our energy, and since both $p_\parallel$ and y variables exhibit significant variations with energy it is difficult to make a detailed comparison in these variables. The x variable, on the other hand, is seen to be almost energy-independent, and therefore we can use the results from the 9.3-GeV $(\gamma p,\pi^-)$ experiment.[2]

For a comparison between the γd and γp data we have studied the following ratio:

$$R_c = [F_{\gamma d,\pi^-}(x) - F_{\gamma p,\pi^-}(x)]/F_{\gamma p,\pi^-}(x). \qquad (11)$$

Under the assumption of Eq. (2), this ratio is equal to $F_{\gamma n,\pi^-}(x)/F_{\gamma p,\pi^-}(x)$. As seen from Fig. 6, R_c is large for the region $x<-0.5$ and approaches the value of 10 at $x\simeq -1$. For $x>-0.5$, the ratio R_c falls off rapidly and is close to unity in the pionization region. It is worthwhile to note that at x close to 1, R_c falls even somewhat below unity ($\Delta R_c \lesssim \pm 0.10$ in this region).

Assuming factorization, it has been suggested that the relation $(\gamma n,\pi^-)=(\gamma p,\pi^+)$ holds for $x<-0.5$,[13] since we are in the target fragmentation region. The feature that R_c drops off sharply at $x\simeq -0.5$ has been explained by Horn[13] to arise because this is the edge of the "pure" target fragmentation region. By "pure" we mean that a particle with $|x|>0.5$ is the leading particle in either beam or target direction. Note that the relation $(\gamma n,\pi^-)=(\gamma p,\pi^+)$ holds even if the isoscalar-isovector interference term of the photon exists. Thus the ratio R_c in this region is equal to $F_{\gamma p,\pi^+}(x)/F_{\gamma p,\pi^-}(x)$. In fact, the ratio $F_{ap,\pi^+}(x)/F_{ap,\pi^-}(x)$, where a is any incoming particle, should be independent of the beam particle in the region $x<-0.5$ under the assumption of factorization. The data available at present for $a=p$ (Ref. 14) and $a=\pi^+$ (Ref. 15) seem to support this result. Both data give a ratio of approximately 10 near $x\simeq -1$. Our calculation of the ratio for $a=\gamma$ gives a similar value at $x\simeq -1$, which confirms the above results.

In the region $x\simeq 1$, i.e., the beam fragmentation

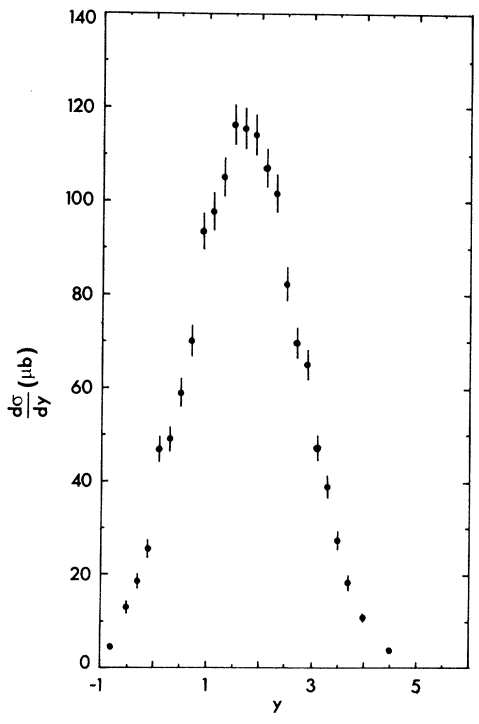

FIG. 5. The π^- cross section $d\sigma/dy$ versus y.

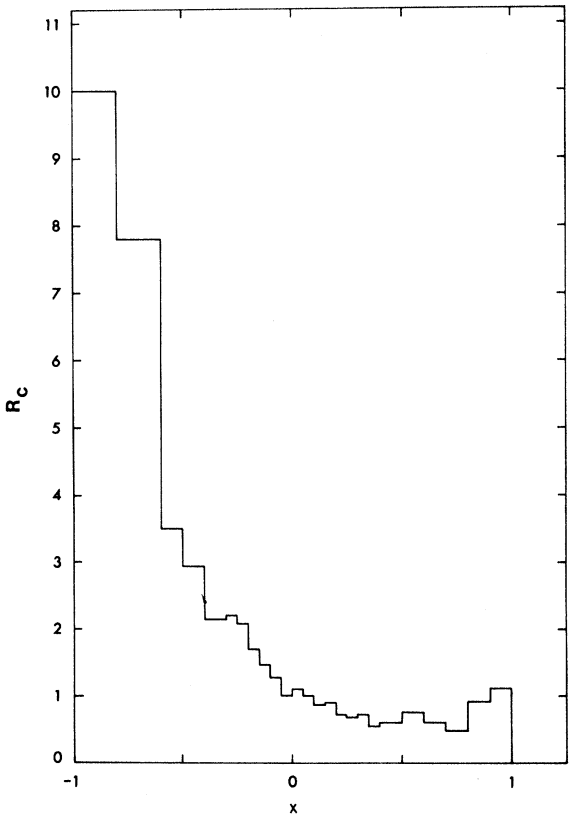

FIG. 6. The ratio $R_c = F_{\gamma n,\pi^-}(x)/F_{\gamma p,\pi^-}(x)$.

region, we expect $F_{\gamma n,\pi^-}(x)/F_{\gamma p,\pi^-}(x)$ to be identical to unity. The deviation of the ratio from unity might be due to the fact that in this region the contribution from the coherent $(\gamma d_c, \pi^-)$ events is not negligible, and thus the assumption of Eq. (2) is less justified.

In order to compare our π^- spectrum with those spectra obtained in hadronic reactions, following Chan Hong-Mo *et al.*[16] we have normalized the distributions by dividing them by their respective asymptotic total cross sections. In Fig. 7 we present a comparison of normalized $F(x)$ distributions between our data using $\sigma_T^{\gamma d}(\infty) = 2\sigma_T^{\gamma p}(\infty)$ and data on π^- production in $\pi^+ p$, $\pi^- p$ (Ref. 17) and γp (Ref. 2) reactions. As can be seen, at negative x our data points lie considerably higher than those of the other experiments, a phenomenon observed in the previous figure. At positive x our data follow the nonexotic channels. If the coherent $(\gamma d_c, \pi^-)$ behaved like an exotic channel, and had a non-negligible contribution, we would have expected the curve to approach the $(\pi^+ p, \pi^-)$ data points.

In Fig. 8 we compare the normalized $[1/\sigma_T(\infty)] \times d\sigma/dp_\parallel$ with our data for the reactions (ap, π^-), where $a = p$, K^+, π^+, π^- (Ref. 18), and γ (Ref.2). The same effect manifested in the previous figure can also be noted here, i.e., at low $p_\parallel$ our data points are consistently higher than the other data, and at higher $p_\parallel$ our points are essentially following the nonexotic channels.

Chang Hong-Mo *et al.*[19] predicted $F_{\gamma p,\pi^+}(p_\parallel)$ to be similar in magnitude to $F_{\gamma p,\pi^-}(p_\parallel)$ at small and

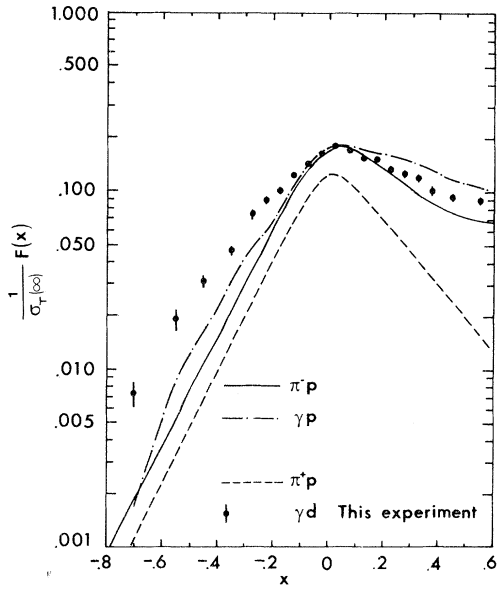

FIG. 7. The normalized structure function $F(x)/\sigma_T(\infty)$ versus x. The curves are approximations of other photoproduction and hadron π^- inclusive data.

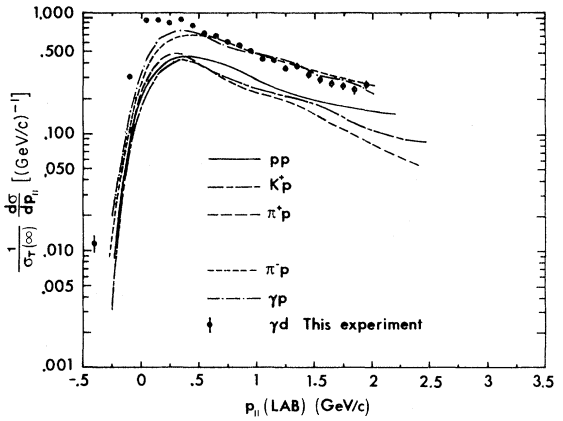

FIG. 8. The normalized structure function $F(p_\parallel)/\sigma_T(\infty)$ versus $p_\parallel$. The curves are approximations of other photoproduction and hadron π^- inclusive data.

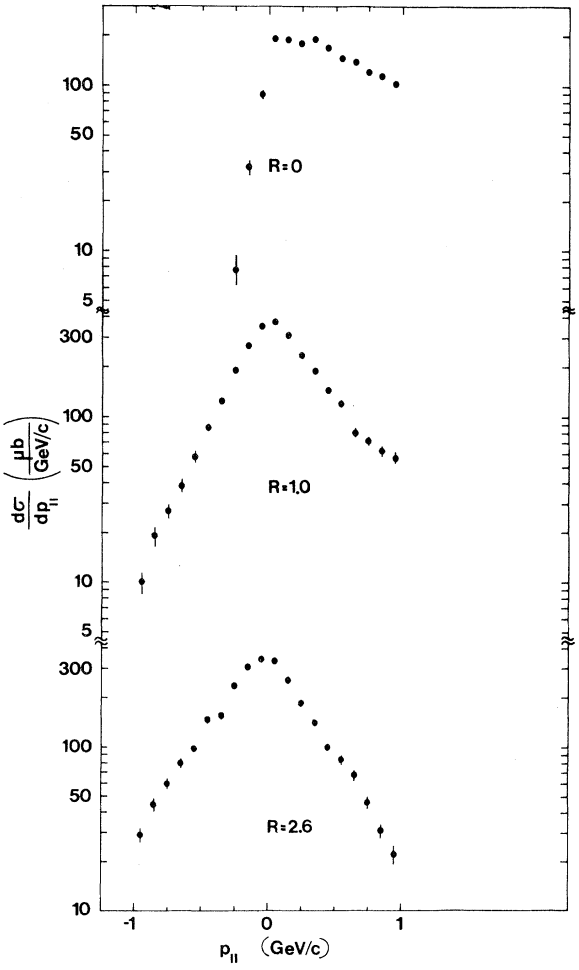

FIG. 9. The longitudinal-momentum distribution $p_\parallel$ calculated at different values of $R = p_{\text{proton}}/p_{\text{photon}}$. (a) $R = 0$; (b) $R = 1$; (c) $R = 2.6$.

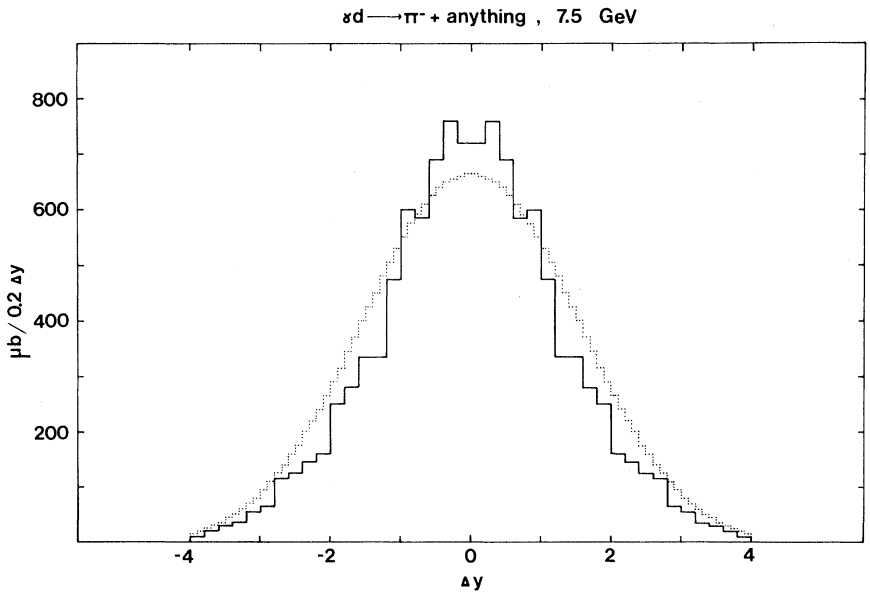

FIG. 10. Correlation terms in y. The solid-line histogram is the coincidence $d^2\sigma/dy_1 dy_2$ distribution. The dotted histogram is the normalized product of the inclusive one-π^- distribution $(1/N)$ $(d\sigma/dy_1)$ $d\sigma/dy_2$.

negative $p_{\parallel}$. Our result that the normalized $F_{\gamma d,\pi^-}(p_{\parallel})$ is greater than the normalized $F_{\gamma p,\pi^-}(p_{\parallel})$ by a factor of approximately 5 implies, under the assumption of Eq. (2), that $F_{\gamma n,\pi^-}(p_{\parallel})$ is greater than $F_{\gamma p,\pi^-}(p_{\parallel})$ by an order of magnitude. Since $F_{\gamma n,\pi^-}(p_{\parallel}) \simeq F_{\gamma p,\pi^+}(p_{\parallel})$ at $p_{\parallel}$ small and negative, our results contradict the prediction of Chang Hong-Mo *et al.*

The asymmetry of the longitudinal momentum $p_{\parallel}$ distribution is a function of the reference frame where it is calculated. Elbert *et al.*[20] have studied the $p_{\parallel}$ distribution in $(\pi^- p, \pi^{\pm})$ reactions and found that the longitudinal momentum distribution is symmetric in a reference frame where the ratio R of the target and beam momenta equals 1.5. This result has been interpreted[20] as arising from the symmetry in the quark-quark c.m. system for the quark-quark collision that takes place. In the $(\gamma p, \pi^-)$ experiment,[2] this ratio was found to be close to $R \sim 3$, and, in the spirit of quark-quark

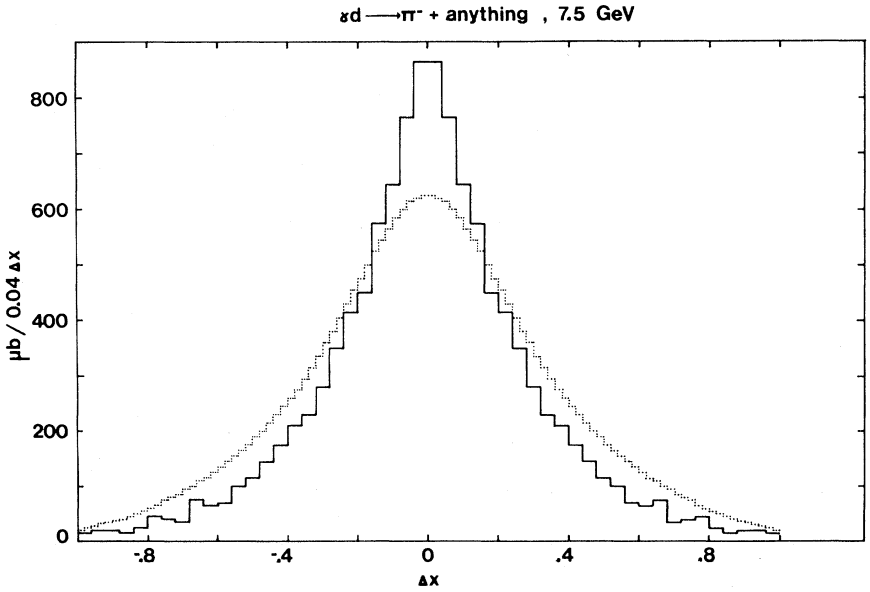

FIG. 11. Correlation terms in x. The solid-line histogram is the coincidence $d^2\sigma/dx_1 dx_2$ distribution. The dotted histogram is the normalized product of inclusive one-π^- distribution $(1/N)$ $(d\sigma/dx_1)$ $d\sigma/dx_2$.

interactions, it suggested that the photon interacts as a single quarklike object. In Fig. 9 we show the $d\sigma/dp_{\parallel}$ distribution, where $p_{\parallel}$ is calculated for three values of R in the γ-nucleon system, namely $R=0$ (laboratory system), $R=1$ (c.m. system), and $R=2.6$, where the data were found to exhibit a symmetric distribution. This value of $R=2.6$ is in good agreement with the result found in $(\gamma p, \pi^-)$.[2] We have also calculated the $p_{\parallel}$ distributions for different values of R in the γd system and found them to be symmetric at $R \simeq 4$. Assuming the photon to interact as a single quark with the deuteron nucleus as a whole, one would expect R to be ≈ 6.

V. CORRELATIONS

Additional information on the outgoing π^- particles may be obtained by studying correlations between the particles in different variables. In general, two-particle correlations in any variable are defined by the function

$$g(v_1, v_2) = \frac{d^2\sigma}{dv_1 dv_2} - \frac{1}{N}\frac{d\sigma}{dv_1}\frac{d\sigma}{dv_2}, \tag{12}$$

where v_1 and v_2 are the variables under investigation for the first and second π^-, respectively; N is a renormalization factor such that when v_1 and v_2 are uncorrelated the integral of $g(v_1, v_2)$ is equal to zero. In the evaluation of the function $g(v_1, v_2)$ we calculated in the first term the coincidence of the particles from the same event. The second term is the product of the v_1 and v_2 distributions of all π^- produced. In these distributions events with single-π^- production were included as well.

In Fig. 10 we show the two terms of the correlation function (12) for the rapidity variable. The solid-line histogram shows the coincidence of the two π^- when their rapidities are Δy apart. The dotted histogram is the second term in the expression (12). The difference between the two histograms measures the amount of correlation in this variable. In Fig. 11 similar distributions in the x variable are shown. Here too the solid and dotted histograms represent the first and second terms of Eq. (12). As seen in both figures, one finds correlations in both variables, where the correlation in the x variable is more significant. In both cases positive correlations near $\Delta x, \Delta y = 0$ is seen, which turn negative at larger values of $|\Delta x|, |\Delta y|$. A similar behavior of the rapidity variable has been observed by Ko in his study of the π^- inclusive production in $K^+ p$ interactions at 12 GeV/c.[21]

VI. CONCLUSIONS

In summary, we have found the assumption that $(\gamma d, \pi^-)$ behaves as the sum of $(\gamma p, \pi^-)$ and $(\gamma n, \pi^-)$ to yield resonable results.

The γn average charge multiplicity was found to be 2.7 ± 0.2, which is one unit of charge less than the γp average charge multiplicity.

The ratio $F_{\gamma n, \pi^+}(x)/F_{\gamma p, \pi^-}(x)$ in the target fragmentation region is equal to both $F_{pp, \pi^+}(x)/F_{pp, \pi^-}(x)$ and $F_{\pi^+ p, \pi^+}(x)/F_{\pi^+ p, \pi^-}(x)$. This equality is expected if one assumes factorization to hold.

We found that the $p_{\parallel}$ distribution is symmetric in a frame where $R \simeq 2.6$, suggesting that the photon interacts like a single quark.

Both the x and y variables exhibit positive correlation near $\Delta x, \Delta y = 0$, and the x variable seems to be a more sensitive variable for such a study.

VII. ACKNOWLEDGMENTS

We thank D. Horn for many fruitful discussions. We are also indebted to Y. Oren for his help in the early stage of this experiment. The cooperation of SLAC in the performance of this experiment is gratefully acknowledged. In particular, we are indebted to J. Ballam and G. B. Chadwick. Our thanks are also due to R. Watt and the SLAC Bubble Chamber Operation crew, and the SLAC Research Areas Division personnel.

Finally, we would like to acknowledge the valuable help of our technical and scanning staff at Tel Aviv.

---

*Present Address: Institute for High Energy Physics of the Austrian Academy of Science, Vienna, Austria.

†Address after January 15, 1973: Laboratory of Nuclear Science, Massachusetts Institute of Technology, Cambridge, Massachusetts 02139.

[1]For a review, see e.g. E. L. Berger, ANL Report No. ANL/HEP 7148 (unpublished); W. Frazer *et al.*, Rev. Mod. Phys. 44, 284 (1972); D. Horn, Phys. Reports 4C, 1 (1972).

[2]K. C. Moffeit *et al.* (SLAC-Berkeley-Tufts Collaboration), Phys. Rev. D 5, 1603 (1972).

[3]See e.g. B. Wiik, in *Proceedings of the International Symposium on Electron and Photon Interactions at High Energies*, edited by N. B. Mistry (Cornell Univ. Press, Ithaca, N.Y., 1972), p. 163.

[4]H. Braun *et al.*, Phys. Rev. D 6, 2311 (1972); M. A. Ijaz *et al.*, Nucl. Phys. B42, 85 (1972).

[5]Y. Eisenberg *et al.*, Nucl. Phys. B42, 349 (1972).

[6]See e.g. K. G. Wilson, Cornell Report No. CLNS-131, 1970 (unpublished).

[7]J. J. Murray and P. Klein, SLAC Report No. SLAC-TN-67-19 (unpublished).
[8]T. M. Knasel, DESY Report No. DESY 70/3 (unpublished).
[9]D. O. Caldwell *et al.*, Phys. Rev. Letters 25, 609 (1970); 25, 613 (1970).
[10]R. P. Feynman, Phys. Rev. Letters 23, 1415 (1969).
[11]J. Benecke *et al.*, Phys. Rev. 188, 2159 (1969).
[12]C. E. DeTar, Phys. Rev. D 3, 128 (1971).
[13]D. Horn, Tel-Aviv Report No. TAUP-271-72R (unpublished).
[14]J. V. Allaby *et al.*, CERN Report No. 70-12, 1970 (unpublished).
[15]J. V. Beaupre *et al.*, Phys. Letters 37B, 432 (1971).
[16]Chan Hong-Mo *et al.*, Phys. Rev. Letters 26, 672 (1971).
[17]W. D. Shephard *et al.*, Phys. Rev. Letters 27, 1167 (1971).
[18]M. -S. Chen *et al.*, Phys. Rev. Letters 26, 1585 (1971).
[19]Chang Hong-Mo *et al.*, Phys. Letters 40B, 112 (1972).
[20]J. Elbert *et al.*, Phys. Rev. D 3, 2042 (1971).
[21]W, Ko, Phys. Rev. Letters 28, 935 (1972).

PHYSICAL REVIEW D VOLUME 8, NUMBER 3 1 AUGUST 1973

New Determination of the Dalitz-Plot Distribution for τ^- Decays*

P. W. Lucas,† H. D. Taft, W. J. Willis
Yale University, New Haven, Connecticut 06520
(Received 13 November 1972)

We have measured the X and Y projections of the Dalitz plot of 81 000 τ^- decays. The decays were observed in a beam of 400-MeV/c K^-'s in the BNL 30-in. liquid-hydrogen bubble chamber. For the X distribution we find no deviation from phase space. For Y we find a distribution of (phase space) $\times(1+AY)$ and have determined for A the values 0.252 $\pm$ 0.011 with Coulomb corrections to the distribution, 0.219 $\pm$ 0.011 without Coulomb corrections. The results have been obtained using a method which involves measured rather than fitted quantities.

I. INTRODUCTION

The distribution of the Dalitz plot for charged K mesons decaying via the τ mode,

$$K^\pm \to \pi^\pm \pi^\pm \pi^\mp ,$$

should be a property of the weak interaction measurable with a minimum of experimental difficulty. The decay can be observed in a bubble chamber or in a counter system, with all tracks, both incoming and outgoing, charged and observable. For K^+ the decays can be observed for particles at rest, while for K^- they must be observed in flight to avoid nuclear absorption. The distribution is experimentally well represented by three-body phase space (flat Dalitz plot) multiplied by a term linear in the kinetic energy of the odd pion. There is some evidence stated for more involved structure,[1,2] but none has been convincingly proved.

Despite the apparent simplicity of the problem, the precise measurement of the slope of the linear term, the only measured quantity needed to describe the distribution within the accuracy of current experiments, has been difficult and has given inconsistent results previously. It was in an attempt to resolve this inconsistency that the experiment reported here was performed.

II. DALITZ PLOT

We have chosen to parametrize the Dalitz plot in terms of the variables X and Y defined by

$$X = \frac{\sqrt{3}}{Q}\,|T_1 - T_2|, \qquad Y = \frac{1}{Q}(3T_3 - Q),$$

where T_1 and T_2 are the kinetic energies in the K^- center-of-mass system of the two π^-, T_3 is the kinetic energy of the π^+, and Q is the energy release of the decay, given by

$$Q = M_K - 3M_\pi$$
$$= 75.09 \pm 0.12 \text{ MeV}.$$

In terms of these variables the Dalitz plot is bounded by the closed curve formed by the Y axis and the curve

$$X = +\left[\frac{2M_K Q Y^3 + (4M_\pi^2 - 2QM_K + Q^2)Y^2 - (2M_K - Q)^2}{Q^2 Y^2 + 2Q(3M_\pi - Q)Y - 4M_\pi^2 + 2QM_\pi - Q^2}\right]^{1/2}.$$